# An approach to reseach of the breaching process

Weij, Dave; Keetels, Geert; Goeree, Joep; van Rhee, Cees

**Publication date**
2016

**Document Version**
Final published version

**Published in**
Proceedings of the 21st World Dredging Congress & Exhibition 2016 (WODCON XXI)

**Citation (APA)**
Weij, D., Keetels, G., Goeree, J., & van Rhee, C. (2016). An approach to reseach of the breaching process. In *Proceedings of the 21st World Dredging Congress & Exhibition 2016 (WODCON XXI): Innovations in Dredging* (Vol. 2, pp. 821-833). Western Dredging Association.

# AN APPROACH TO RESEARCH OF THE BREACHING PROCESS

D. Weij[1], G. H. Keetels[2], J. Goeree[3] and C. van Rhee[4]

## ABSTRACT

Breaching has been an important mechanism for sand suction dredging for a long time. A special kind of breaching, unstable breaching, has recently been identified as a possible failure mechanism for sandy submerged slopes. This has increased the interest into the breaching process. At the Delft University of Technology we have started a research project on the subject of unstable breaching. In this paper we discuss the results obtained so far. First, we discuss a concept for laboratory experiments into the phenomena. Second, we propose a new numerical model, designed to investigate unstable breaching.

**Keywords:** Slope failure, sand-water mixtures, numerical modelling, dredging, turbidity currents, flow slides

## INTRODUCTION

Breaching is an important production mechanism for stationary suction dredgers. Because it caused several large scale slope failures, interest in the mechanism has increased in recent years. Between 2011 and 2014, Beinssen et al. (2014) monitored a stretch of beach adjacent to a tidel inlet in Australia, called Amity Point. They recorded 44 breaching related failure events. The largest of these resulted in the loss of 2980 $m^2$ of beach. In September, 2015, a similar event occured nearby at Inskip Point. A beach collapse resulting in a slowly regressing erosion scarp of eventually 200 meters wide developed, which swallowed part of a camping site. In this case the process was initiated by erosion due to tidal currents, however a breach failure can also be initiated by dredging activity. This occurred, for example, in 2008, in the Dutch town of Staphorst, where dredging activity initiated the breaching process, which resulted in the damage shown in Figure 1 (De Groot and Mastbergen, 2008). Breaching was also identified as a source for large oceanic turbidity currents (Mastbergen and Van Den Berg, 2003; Eke et al., 2011).

**Figure 1. A lake border damaged by the unstable breaching process at Hooidijk, 2008. (Source: D.R. Mastbergen)**

Breaching mostly occurs in dense sandy soils with a low permeability (Van Rhee and Bezuijen, 1998; Mastbergen and Van Den Berg, 2003). The process starts with the formation of a slope, whose angle is steeper then the internal friction angle. This is called the breach face. When breaching is part of sand collection, this steep slope would be created by a suction dredger. A slope steeper than the internal friction angle is not stable, and will start to slide. Dense sand can

[1]PhD student, Delft University of Technology, Mekelweg 2, Delft, Netherlands, T: +3115-278 5524, Email: D.Weij@tudelft.nl

[2]Assistant professor, Delft University of Technology, Mekelweg 2, Delft, Netherlands, T: +3115-278 4057, Email: G.H.Keetels@tudelft.nl

[3]Postdoctoral researcher, Delft University of Technology, Mekelweg 2, Delft, Netherlands, T: +3115-278 3297, Email: J.C.Goeree@tudelft.nl

[4]Professor of Dredging Engineering, Delft University of Technology, Mekelweg 2, Delft, Netherlands, T: +3115-278 3973, Email: C.vanRhee@tudelft.nl

start to expand during sliding, this is called dilatancy. The pore volume increases during dilatancy, which should be compensated by an inflow of water. Therefore, dilatancy is accompanied by a reduction in pore water pressure. This reduced pore water pressure can temporarily keep the steep breach face stable. As water flows in, sand particles are released one by one at the sand-water interface, where they develop into a turbidity current. This results in a steep breach face slowly regressing away from its original position, while releasing sand particles into a turbidity current (Figure 2). This current can be used by the dredgers to collect sand without moving, as the current transports sand toward the suction mouth.

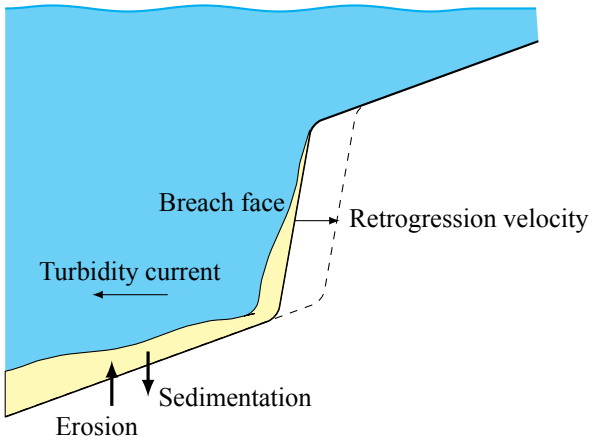


**Figure 2. Schematization of the breaching process .**

A breach can be stable or unstable. During a stable breach, the breach face decreases in size over time, and will quickly disappear. When the breach is unstable, the breach face increases in size over time. When this happens, of the process can go on for a long time, sometimes exceeding a day. The end result can be large sections of land disappearing into the water, as seen in Figure 1.

Whether a breach is stable or unstable depends on the difference of the slopes up- and downstream of the breach face. When the slope that forms downstream of the breach face is milder than the upstream slope, the breach is unstable (See Figure 3). The slope formed downstream of the breach face will depend mostly on the interaction between the formed turbidity current and the existing downstream slope.

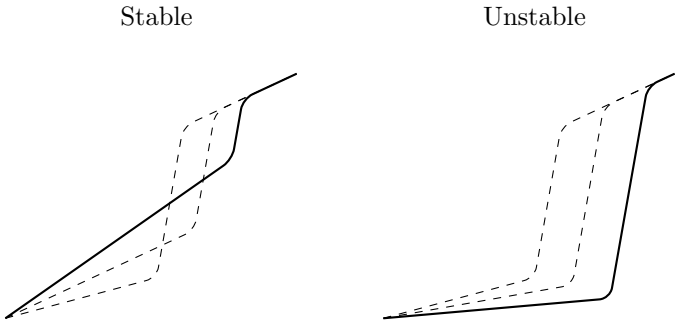


**Figure 3. The difference between stable and unstable breaching.**

Until now, research of the breaching process has mostly taken place in laboratory settings (Breusers, 1977; Van Rhee and Bezuijen, 1998). The scale of laboratory experiments is limited, as large scale tests are costly. However, several phenomena only occur at larger scales (Van Rhee and Bezuijen, 1998). Recently a field test was carried out in the Netherlands, where breach heights of up to 6 meters were observed (Mastbergen et al., 2015). These field tests are

costly, and take a lot of preparation time. Numerical models, where the scale can be increased at a much lower cost, are an alternative to laboratory experiments

Numerical investigations with a 1D-model were carried out by Mastbergen and Van Den Berg (2003). While Van Rhee (2015) has investigated the process using a 2D-model. In his model, the soil is modelled using an immersed boundary method combined with formulae for the pickup and sedimentation of sand. The effects of the pore pressure feedback are taken into account by adjusting the pick-up formula at the sand-water interface (Van Rhee, 2010).

To improve our knowledge of the breaching process, we want to extend the model to 3D. Furthermore, we want to investigate the pore pressure feedback mechanism in breaching. To do so, we model the whole domain as one sand-water mixture, with large variations in sand concentration. With this approach, we model both the water and the soil, instead of only the sand-water interface.

We supplement the model with laboratory experiments. To investigate breaching in a laboratory environment, creating the initial steep breach face is important. The standard in experiments is to use a mechanical slide, which is removed at the start of the experiment. The drawback of this method is that the shape of the initial sand column is limited by the position of the mechanical slide. To avoid this drawback, we came up with the idea to use a pump to temporarily keep the sand in place. We test this idea first in a small scale setup, with the aim of applying it to larger experiments at a later stage, if shown to be successful.

In this paper we describe this small scale laboratory setup. We also describe the soil model of our new numerical model, which can later be extended to include the pore pressure feedback mechanism. This forms the basis for our research of the unstable breaching process.

## LABORATORY EXPERIMENTS

In this section we describe a new method to initialize experiments with sand, which use an initial slope steeper than its angle of repose. We describe the small scale setup, give some theoretical backgrounds, and show the setup in action.

### Setup Description

A schematic side view of the setup is shown in Figure 4. We use a basin made of 20 mm thick acrylic glass with a size of 1.08 m $\times$ 0.97 m $\times$ 0.76 m. An acrylic glass plate, with a height of 0.87 m, separates the basin into two equally sized compartments, A and B (See Figure 4), of 0.54 m $\times$ 0.78 m. In compartment A, we have created a smaller compartment with a width of 0.1 m, closed off with geotextile. A centrifugal pump (Marina SM 98 CR) is connected at the top of this compartment. This pump displaces water from the small compartment to the compartment B. When sand is placed against the geotextile, water is forced to pass trough the sand. A hydraulic gradient is created which keeps the sand stable at angles steeper than the angle of friction. While the pump is on, we can freely modify the shape of the sand profile.

In the middle of compartment A, we placed a sliding gate covered in geotextile. We use this slide to create an initial sand profile in the compartment. This slide is not mandatory part of the setup, it is also possible to initialize the sand at a certain slope.

### Theory

Van Rhee and Bezuijen (1992) investigated the effect of a pressure gradient on the stability of slopes. A tank with inner measurements of 300 mm $\times$ 300 mm $\times$ 600 mm contained a sand bed about 0.1 m thick with a median grain diameter of 200 µm. By connecting the areas above and below the sample with water reservoirs with different water levels, an upward or downward flow through the sample was established. A given head difference over the sand bed was imposed, and the tank was rotated until the sand started moving. Their results show a clear relation between hydraulic gradient and the steepest possible slope. They derived for the slope, $\beta$, that is just stable

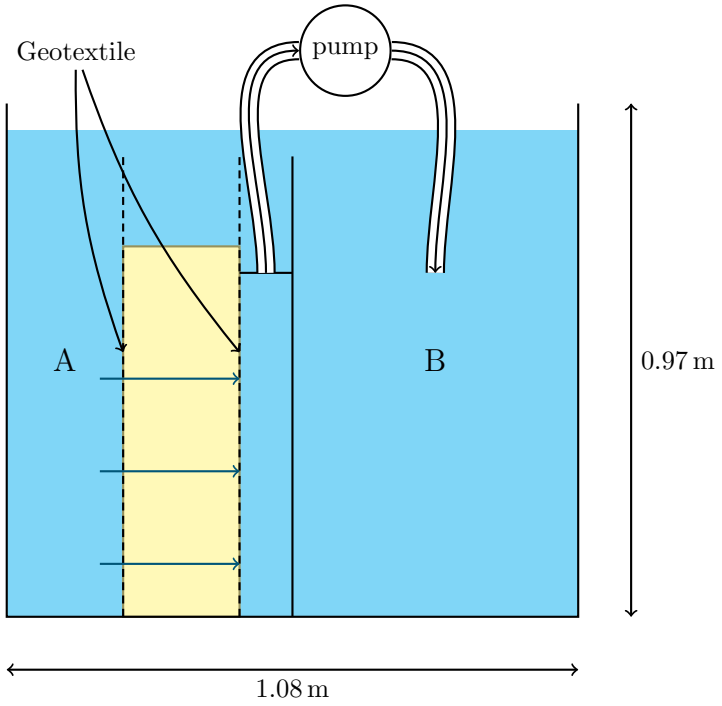


**Figure 4. Schematic side view of the experimental setup.**

$$\beta = \phi + \arcsin\left(\frac{3i\sin\phi}{4\Delta}\right) \tag{1}$$

where $\phi$ is the internal friction angle, $i$ is the hydraulic gradient, and $\Delta$ is the relative grain density. This can be rewritten to find the necessary hydraulic gradient to keep a slope stable

$$i = \frac{4}{3}\Delta\frac{\sin(\beta-\phi)}{\sin\phi} \tag{2}$$

We use a pump to create this hydraulic gradient. Using the calculated hydraulic gradient, the necessary discharge of the pump can be determined using the Darcy formula (Darcy, 1856).

$$Q = Aki \tag{3}$$

where $Q$ is the discharge in $\mathrm{m}^3/\mathrm{s}$, $A$ is the cross section of the sand block in $\mathrm{m}^2$, and $k$ is the permeability of the sand in $\mathrm{m}/\mathrm{s}$. For our test set-up, we used sand with a permeability around $1 \times 10^{-4}\,\mathrm{m}/\mathrm{s}$. This leads for to a pump discharge of $1.05 \times 10^{-4}\,\mathrm{m}^3/\mathrm{s}$, with a required pressure difference of roughly one meter water column. For larger permeabilities or cross sections, the necessary discharge increases.

**Results**

The setup in action is shown in Figure 5. Here the pump is turned on and the sheet of geotextile on the left of the sand is removed. While the pump was left on, the sand remained in the same position. When the pump was turned off, the sand started flowing as expected.

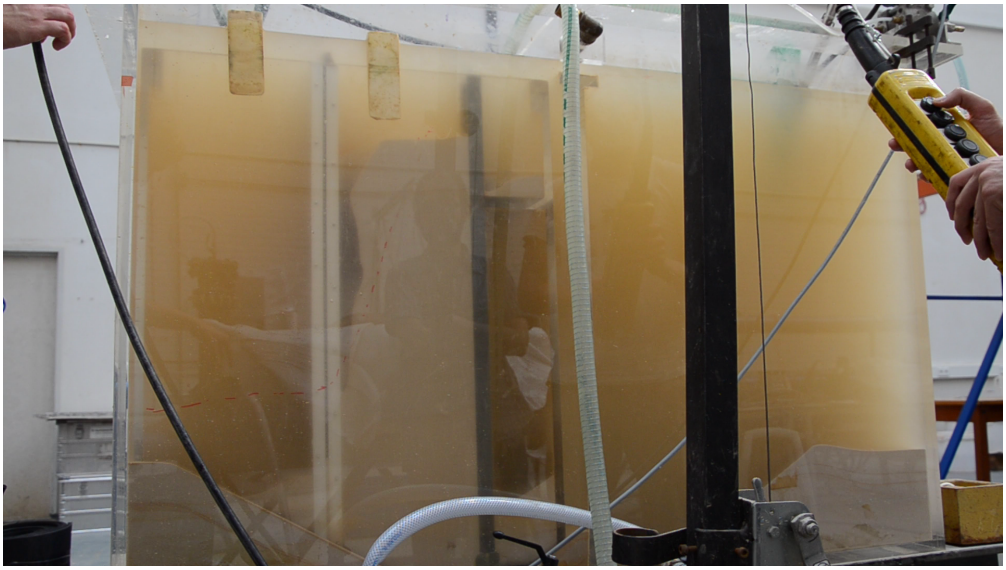

**Figure 5. The laboratory setup in action.**

We have also managed to initiate a slope with a slope of 55 degrees (Figure 6). Again, the sand remained stable as longs as the pump was turned, as shown in Figure 6a. When the pump was turned off, the failure of the slope started, as seen in Figure 6b. As in the breaching process particles slowly release at the surface of the slope and flow downward. Because of the wall, the particles settle at the foot of the initial slope, forming a new slope with an angle milder than the internal friction angle. Figure 6c shows the final state of the experiment. The end result is a new slope with an angle milder than the internal friction angle.


**Figure 6. Initialization of a slope of 55 degrees before turning off the pump (a), 30 seconds after turning off the pump (b) and two minutes after (c).**

## NUMERICAL MODEL

In this section, we describe our numerical model. We limit ourselves to modelling dense granular flow submerged in water, which is an essential first step in modelling the breaching process. In the future, the model will be expanded to include the pore pressure feedback mechanism.

It is common practice not to model the dense friction dominated region, and instead use an immersed boundary at the transition between these two domains. Common practice is to use an immersed boundary at the interface between the sand bed and the water. At this immersed boundary, formulae for erosion and sedimentation are applied. However, in this approach, phenomena inside the sand bed are strongly simplified, while in our case these phenomena play an important role. To increase insight into what happens in the sand bed, we model the whole domain as one sand-water mixture, with large variations in sand concentration. In the friction dominated sand bed, the mixture does not act as a Newtonian fluid, and the standard Navier-Stokes equations are therefore no longer valid. Instead the material remains rigid, unless the shear stresses inside the material exceed a yield stress. The necessary yield shear stress for motion depends the pressure between sand particles. A larger pressure leads to a higher yield stress. For the flow after the

initiation of movement, we use the $\mu(I)$ rheology of GDR MiDi (2004).

**Drift-flux Model**

In our study, we used the drift-flux model of OpenFOAM version 2.3.0 as the basis for our model (Brennan, 2001). The drift-flux model is derived by starting from balance equations for multiphase flow, for example those of Jackson (1997). In the framework of Jackson (1997), there are separate mass and momentum balance equations of the continuous phase and the dispersed phase (In our case we have a water and sand phase). In the drift-flux model, these balance equations are summed to arrive at single mass and momentum balance equations for the complete mixture. A full derivation of these equations can be found in Manninen et al. (1996).

The continuity equation is given by

$$\frac{\partial \rho_m}{\partial t} + \nabla \cdot (\rho_m \boldsymbol{u}_m) = 0 \tag{4}$$

Where $\rho_m$ is the mixture density, and $\boldsymbol{u}_m$ is the velocity of the centre of gravity of the mixture. These are defined as follows

$$\rho_m = \sum_{k=1}^{n} \alpha_k \rho_k \tag{5}$$

$$\boldsymbol{u}_m = \frac{1}{\rho_m} \sum_{k=1}^{n} \alpha_k \rho_k \boldsymbol{u}_k \tag{6}$$

Where $\boldsymbol{u}_k$ is the velocity of phase $k$, and $\rho_k$ the density of phase k (in our case a water and sand phase).

The momentum equation is

$$\frac{\partial}{\partial t} \rho_m \boldsymbol{u}_m + \nabla \cdot (\rho_m \boldsymbol{u}_m \boldsymbol{u}_m) = -\nabla p_m + \nabla \cdot \left( \underline{\underline{\boldsymbol{\tau}}}_m + \underline{\underline{\boldsymbol{\tau}}}^{\mathrm{t}}_m + \underline{\underline{\boldsymbol{\tau}}}^{\mathrm{D}}_m \right) + \rho_m g + \boldsymbol{M}_m \tag{7}$$

The term $\boldsymbol{M}_m$ is the influence of the surface tension force on the mixture, which can be taken as zero in the case of solid particles. The term $p_m$ is the mixture pressure, and is equal to the linear combination of the dispersed phase and continuous phase pressures. The term $\underline{\underline{\boldsymbol{\tau}}}^{\mathrm{D}}_m$ represents the diffusion stress due to the differences between phase velocities and mixture velocity.

$$\underline{\underline{\boldsymbol{\tau}}}^{\mathrm{D}}_m = \sum_{k=1}^{n} \alpha_k \rho_k \left( \boldsymbol{u}_k - \boldsymbol{u}_m \right) \left( \boldsymbol{u}_k - \boldsymbol{u}_m \right) \tag{8}$$

The phase velocities, $\boldsymbol{u}_k$ are not calculated in the drift flux model. Therefore, the diffusion stress, $\underline{\underline{\boldsymbol{\tau}}}^{\mathrm{D}}_m$, is rewritten in terms of the drift-flux of the dispersed phase, $\boldsymbol{v}_{dj}$. The drift flux velocity is the difference between the velocity of a phase and the volumetric flux of the mixture. The volumetric flux, $\boldsymbol{j}$, is the velocity of the volume centre and is defined as

$$\boldsymbol{j} = \sum_{k=1}^{n} \alpha_k \boldsymbol{u}_k \tag{9}$$

Where $\alpha_k$ is the volume concentration of phase $k$.

The drift flux of the dispersed phase is thus defined as

$$\boldsymbol{v}_{dj} = \boldsymbol{u}_d - \boldsymbol{j} \tag{10}$$

To close the system, this drift flux has to be determined. The drift flux model assumes that a local equilibrium drift-flux will be established over relatively short length scales. This assumption is correct for small particles ($D < 200\,\mu\text{m}$) (Manninen et al., 1996). In this case, we can apply the terminal velocity without a significant error. We determine the drift-flux of the dispersed phase with the formula of Richardson and Zaki (1954)

$$\boldsymbol{v}_{dj} = w_0 \left(1 - \alpha_d\right)^n \tag{11}$$

where $w_0$ is the settling velocity for $\alpha_d = 0$ and $n$ is the Richardson-Zaki hindered settling exponent [-]

Based on the experiments of Richardson and Zaki (1954), Rowe (1987) gives an empirical formula to estimate the Richardson-Zaki exponent, $n$

$$n = 2.35\frac{2 + 0.175Re_p^{0.75}}{1 + 0.175Re_p^{0.75}} \tag{12}$$

Where $Re_p$ is the Reynolds number for an isolated particle at terminal velocity. Changes in the sand concentration, $\alpha_d$, are governed by the continuity equation of the dispersed phase. This is rewritten using the mixture velocity, $\boldsymbol{u}_m$, and the drift flux velocity, $\boldsymbol{v}_{dj}$, giving

$$\frac{\partial}{\partial t}\left(\alpha_d \rho_d\right) + \nabla\cdot\left(\alpha_d \rho_d \boldsymbol{u}_m\right) = -\nabla\cdot\left(\alpha_d \frac{\rho_c}{\rho_m}\boldsymbol{v}_{dj}\right) \tag{13}$$

**Rheology**

The original drift-flux model is suitable for concentrations up to 30% (Van Rhee, 2002). The effects of friction are included to make the model suitable for dense granular matter as well.

***Describing the Soil as a Bingham Fluid***

We propose to model the sand bed as a Bingham fluid. Lalli and Di Mascio (1997) were one of the firsts to propose this approach. In the Bingham rheology the shear stress tensor, $\underline{\underline{\boldsymbol{\tau}}}$, is defined as.

$$\begin{array}{ll} \dot{\gamma} = 0 & \text{if } \tau \leq \tau_y \\ \underline{\underline{\boldsymbol{\tau}}} = \left(\frac{\tau_y}{\dot{\gamma}} + \mu\right)\boldsymbol{\gamma} & \text{if } \tau > \tau_y \end{array} \tag{14}$$

Here $\mu_c$ is the dynamic viscosity of water in Pa s, $\dot{\gamma}$ is the second invariant of the deformation tensor, $\underline{\underline{\boldsymbol{\gamma}}}$, and, using the Einstein summation convention, is defined as follows

$$\dot{\gamma} = \sqrt{0.5\gamma_{ij}\gamma_{ij}} \tag{15}$$

and

$$\underline{\underline{\gamma}} = \gamma_{ij} = \frac{\partial u_i}{\partial x_j} + \frac{\partial u_j}{\partial x_i} \tag{16}$$

When the shear stress is below a given yield stress, $\tau_y$, there is no shear flow. When the shear stress is larger than the yield stress, the stress tensor is given by Equation (14). Similar to Lalli and Di Mascio (1997), we apply the well known yield stress of Coulomb:

$$\tau_y = c + p_d \tan\phi \tag{17}$$

where $p_d$ is the dispersed phase pressure, $\phi$ is the internal friction angle, and $c$ is the cohesion of the soil.

The Bingham framework cannot be applied directly in a numerical method. Usually the Bingham fluid is applied by using an effective viscosity, $\mu_{\text{eff}}$,

$$\mu_{\text{eff}} = \frac{\tau_y}{\dot{\gamma} + \epsilon} + \mu_c \tag{18}$$

To avoid division by zero, a small regularization parameter, $\epsilon$ is added. This means that when the shear stress is below the yield stress, $\tau_y$, there is still a small amount of flow.

$\mu(I)$ ***Rheology***

The Mohr-Coulomb rheology describes at what shear stress the material starts to flow. However, it does not include what happens during failure. GDR MiDi (2004) investigated the results of experiments and discrete particle simulations of different dense granular flows in air. Based on these results, they introduced the inertial number, $I$. They found that the ratio between dispersed phase pressure, $p_d$ and shear stress $\boldsymbol{\tau}$ depends mostly on this inertial number.

$I$ is the ratio between the macro and micro time scales of granular shear flow. A visualization of these time scales is shown in Figure 7. The macro time scale is related to the time it takes for a grain to move past another grain. The micro time scale is related to the time it takes for vertical rearrangement of a particle.

The macro timescale is the reciprocal of the shear rate, $\dot{\gamma}$

$$T_{\text{macro}} = \frac{1}{|\dot{\gamma}|} \tag{19}$$

The micro timescale increases with the diameter, $D$, of the sand grains, as more distance has to be covered for rearrangement. The micro timescale is also related to the force used for rearrangement, this is the dispersed phase pressure, $p_d$. Furthermore, the timescale increases with increasing density of the sand, $\rho_d$, due to inertia. Taking dimensions into account we get the following micro timescale

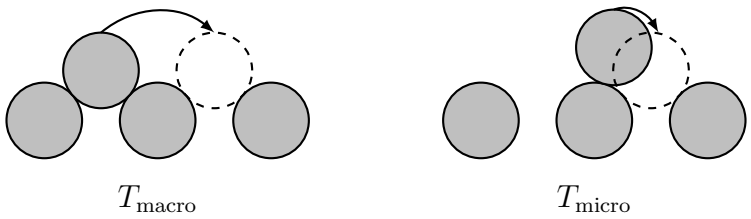


**Figure 7. Schematic showing the physical meaning of the macro and micro time scales [Based on GDR MiDi (2004)].**

$$T_{\text{micro}} = D\sqrt{\frac{p_d}{\rho_d}} \tag{20}$$

Thus, $I$ is defined as

$$I = \frac{T_{\text{micro}}}{T_{\text{macro}}} = \frac{|\dot{\gamma}|\, D}{\sqrt{p_d/\rho_d}} \tag{21}$$

In submarine flows, the interstitial fluid plays an important role in the flow. Cassar et al. (2005) investigated submarine flows of granular materials down a rough incline. They found that the flow can still be described by the inertial number if a micro time scale is chosen which takes the effect of interstitial fluid into account. The alternative time scale is based on the work of Courrech du Pont et al. (2003). The driving force behind the reorganization is still the dispersed phase pressure, $p_d$. However, the retarding effect is due to the viscosity of the interstitial fluid, $\mu_c$, instead of the density. The micro timescale and inertial number for viscous flows is

$$T_{\text{micro,v}} = \frac{p_d}{\mu_c} \tag{22}$$

$$I_v = \frac{\mu_c \dot{\gamma}}{p_d} \tag{23}$$

For higher particle Reynolds numbers ($Re_p > 2.5$), inertia effects become more important than the effects of viscosity. The inertial number in this regime is.

$$T_{\text{micro,i}} = \frac{1}{D\sqrt{\frac{2\rho_c C_d}{3p_d}}} \tag{24}$$

$$I_i = \frac{\dot{\gamma} D\sqrt{2C_d}}{\sqrt{3p_d/\rho_c}} \tag{25}$$

Where $C_d$ is the drag coefficient of a sand particle.

Because $I$ is a local parameter it cannot take into account non-local effects such as arching or grain clusters. However, this rheology seems to be able to accurately predict many different types of granular flows (Cassar et al., 2005; Jop

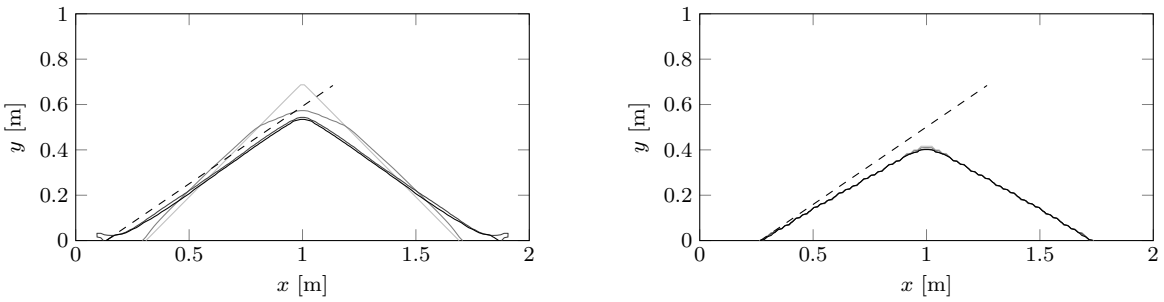


**(a) Initial angle: 45°** **(b) Initial angle: 30°**

**Figure 8. The bed with sand with an internal angle of repose of 35 degrees, for an initial bed of *(a)* 45 and *(b)* 30 degrees. Profiles are shown at intervals of 1 second, darker profiles indicate a later time. Profiles up to 3 seconds are shown. The dashed line indicates the internal friction angle.**

et al., 2006; Doppler et al., 2007; Jop, 2008; Lagrée et al., 2011). Jop et al. (2006) created a model for flow of granular material based on the results of GDR MiDi (2004) for dry granular flow. They calculate the yield stress as follows,

$$\tau_y = \mu(I) p_d \tag{26}$$

where the friction coefficient $\mu(I)$ is:

$$\mu(I) = \mu_s + I \frac{\mu_2 - \mu_s}{I_0 + I} \tag{27}$$

where $\mu_s$ is the critical friction coefficient at zero shear, while $\mu_2$ is the friction coefficient at maximum shear rate. $I_0$ is a constant which determines how quickly the friction coefficient increases towards $\mu_2$. When $\mu_s$ is chosen as $\tan\phi$, we retain our original Mohr-Coulomb yield stress. When the inertial number, $I$, increases, the ratio, $\mu(I)$, between shear stress and dispersed phase pressure also increases.

**Application**

To test the model, we started with heaps of sand with initial angles of 45 and 30 degrees, and an angle of repose of 35 degrees. The sand was given a density of 2650 kg/m$^3$ and a initial porosity of 0.45. The results are shown in Figure 8.

Figure 8a shows results of the simulation with a starting angle of 45 degrees. The contours of the heap are shown at the start of the simulation, with intervals of 1 second, until 5 seconds after the start. After 5 seconds the sand came to a rest. It can be seen that the sand heap came at rest at an angle slightly below the internal angle of friction of 35.

Figure 8b shows results of a similar simulation but with an initial angle of 30 degrees. It can be seen that in this case there is only a little erosion at the toes of the heap and at the top.

***Discussion***

The results show that we are able to recover the internal fraction angle with the model. When the initial angle of the slope is higher than the internal angle of friction, the soil is unstable and starts to flow. The slope angle reduces until the angle is below the internal friction angle, at which point the flow of material is slowed down. This leads to a heap with an angle just below the internal angle of friction.

When the initial angle of the heap is below the internal friction angle, the heap is stable as is expected. However, we do see a little flow of material at certain points. This can be due to our assumption that the dispersed phase pressure is

isotropic, which is not the case. Also our use of a Cartesian grid could introduce errors, since this leads to a 'staircase' edge of the heap, instead of a straight boundary.

The collapse of the heap takes about 3 seconds. This is in the same order of magnitude as experiments in which collapse of a granular column in water, without pore pressure effects, is investigated (Rondon et al., 2011; Topin et al., 2012; Zhao, 2014). This indicates that the effective viscosity and dynamics calculated by the model is also in the right order of magnitude.

## CONCLUSIONS

In this paper, we laid the ground work for further research on the unstable breaching process. We designed and tested a new method of initiating sand with slopes steeper than the internal angle of repose. With the new method, we are no longer limited by the physical location of a slide in designing experiments. The prototype described in this paper can be scaled up to larger scales.

Furthermore, we created a model that is able to model both fluid as well as dense granular materials. With this model, we are able to reproduce the stability of sand piles at their internal angle of friction, with time scales in the right order of magnitude. There are, however, also certain aspects of dense granular materials that the model does not capture. The dispersed phase pressure is assumed to be isotropic, which is not the case in reality. But we believe that in our case the anisotropy is limited, and thus has a limited influence on the results. We can also not capture non-local effects such as arching or grain clusters.

However, we believe that our model is able to correctly capture the behaviour of dense granular material. It is able to model the transition between dense granular material and water, large deformations, turbidity currents, and granular flows in 3D. We also believe that this model is a good first step towards numerical modelling of the breaching process. The next step will be to include the pore pressure feedback mechanism into the model.

## REFERENCES

Beinssen, K., Neil, D., and Mastbergen, D. (2014). "Field observations of retrogressive breach failures at two tidal inlets in Queensland, Australia". *Australian Geomechanics* 49(3), pp. 55–64.

Brennan, D. (2001). "The numerical simulation of two phase flows in settling tanks". PhD thesis. Imperial College London (University of London).

Breusers, H. (1977). "Hydraulic excavation of sand". *Proceedings International Course in Modern dreding*.

Cassar, C., Nicolas, M., and Pouliquen, O. (2005). "Submarine granular flows down inclined planes". *Physics of fluids* 17, p. 103301. DOI: 10.1063/1.2069864.

Courrech du Pont, S., Gondret, P., Perrin, B., and Rabaud, M. (2003). "Granular Avalanches in Fluids". *Physical Review Letters* 90 (4), p. 044301. DOI: 10.1103/PhysRevLett.90.044301.

Darcy, H. (1856). *Les fontaines publiques de la ville de Dijon*.

De Groot, M. and Mastbergen, D. (2008). *Inscharing Hooijdijk februari 2008, Verklaring en herstel*. Technical report 418361-0012. Deltares.

Doppler, D., Gondret, P., Loiseleux, T., Meyer, S., and Rabaud, M. (2007). "Relaxation dynamics of water-immersed granular avalanches". *Journal of Fluid Mechanics* 577(1), pp. 161–181.

Eke, E., Viparelli, E., and Parker, G. (2011). "Field-scale numerical modeling of breaching as a mechanism for generating continuous turbidity currents". *Geosphere* 7(5), pp. 1063–1076.

GDR MiDi (2004). "On dense granular flows". *European Physical Journal E* 14, pp. 341–365.

Jackson, R. (1997). "Locally averaged equations of motion for a mixture of identical spherical particles and a Newtonian fluid". *Chemical Engineering Science* 52(15), pp. 2457–2469. DOI: http://dx.doi.org/10.1016/S0009-2509(97)00065-1.

Jop, P., Forterre, Y., and Pouliquen, O. (2006). "A constitutive law for dense granular flows". *Nature* 441(7094), pp. 727–730.

Jop, P. (2008). "Hydrodynamic modeling of granular flows in a modified Couette cell". *Physical Review E* 77(3), p. 032301.

Lagrée, P., Staron, L., and Popinet, S. (2011). "The granular column collapse as a continuum: validity of a two-dimensional Navier–Stokes model with a $\mu$ (i)-rheology". *Journal of Fluid Mechanics* 686(1), pp. 378–408.

Lalli, F. and Di Mascio, A. (1997). "A numerical model for fluid-particle flows". *International Journal of Offshore and Polar Engineering* 7(2).

Manninen, D., Taivassalo, V., and Kallio, S. (1996). *On the mixture model for multiphase flow*. Tech. rep. Technical Research Centre of Finland.

Mastbergen, D., Van den Ham, G., Cartigny, M., Koelewijn, A., De Kleine, M., Clare, M., Hizzett, J., Azpiroz, M., and Vellinga, A. (2015). "Multiple flow slide experiment in the Westerschelde Estuary, The Netherlands". In: *Submarine Mass Movements and their Consequences*. Springer, pp. 241–249.

Mastbergen, D. and Van Den Berg, J. (2003). "Breaching in fine sands and the generation of sustained turbidity currents in submarine canyons". *Sedimentology* 50(4), pp. 625–637.

Richardson, J. and Zaki, W. (1954). "The sedimentation of a suspension of uniform spheres under conditions of viscous flow". *Chemical Engineering Science* 3(2), pp. 65–73.

Rondon, L., Pouliquen, O., and Aussillous, P. (2011). "Granular collapse in a fluid: role of the initial volume fraction". *Physics of Fluids* 23, p. 073301.

Rowe, P. (1987). "A convenient empirical equation for estimation of the Richardson-Zaki exponent". *Chemical Engineering Science* 42(11), pp. 2795–2796.

Topin, V., Monerie, Y., Perales, F., and Radjaı, F. (2012). "Collapse Dynamics and Runout of Dense Granular Materials in a Fluid". *Phys. Rev. Lett.* 109 (18), p. 188001. DOI: 10.1103/PhysRevLett.109.188001.

Van Rhee, C. (2002). "On the sedimentation process in a Trailing Suction Hopper Dredger". PhD thesis. Delft University of Technology.

Van Rhee, C. (2010). "Sediment entrainment at high flow velocity". *Journal of Hydraulic Engineering* 136(9), pp. 572–582.

Van Rhee, C. and Bezuijen, A. (1992). "Influence of seepage on stability of sandy slope". *Journal of Geotechnical Engineering* 118(8), pp. 1236–1240.

Van Rhee, C. and Bezuijen, A. (1998). "The breaching of sand investigated in large-scale model tests". In: *Coastal Eengineering Conference*. Vol. 3. American Society of Civil Engineers, pp. 2509–2519.

Van Rhee, C. (2015). "Slope failure by unstable breaching". In: *Proceedings of the Institution of Civil Engineers-Maritime Engineering*. Vol. 168. 2. Thomas Telford Ltd, pp. 84–92.

Zhao, T. (2014). "Investigation of landslide-induced debris flows by the DEM and CFD". PhD thesis. University of Oxford.

## CITATION

Weij, D., Keetels, G.H., Goeree, J.C., van Rhee, C. "An Approach to Research of the Breaching Process" *Proceedings of the Twenty-First World Dredging Congress, WODCON XXI, Miami, Florida*, USA, June 13-17, 2016.

## ACKNOWLEDGEMENTS

This research is supported by Stichting Speurwerk Baggertechniek (SSB), Rijkswaterstaat, and Deltares. The laboratory experiments were carried out by the master student Emal Kamal.

## NOMENCLATURE

| | | |
|---|---|---|
| $\alpha_k$ | Volume concentration of phase $k$ | - |
| $\dot{\gamma}$ | Shear rate | $1/\mathrm{s}$ |
| $\mu(I)$ | Friction coefficient | - |
| $\mu_2$ | Limiting fritction coefficient | - |
| $\mu_{\mathrm{eff}}$ | Effective dynamic viscosity | Pa s |
| $\mu_k$ | Viscosity of phase $k$ | Pa s |
| $\mu_s$ | Critical friction coefficient | - |
| $\rho_k$ | Density of phase $k$ | $\mathrm{kg/m^3}$ |
| $\rho_m$ | Mixture density | $\mathrm{kg/m^3}$ |
| $\tau_y$ | Yield stress | $\mathrm{N/m^2}$ |
| $\underline{\underline{\boldsymbol{\tau}}}_m^{\mathrm{D}}$ | Diffusion stress due to the differences between phase velocities and mixture velocity | $\mathrm{N/m^2}$ |
| $\phi$ | Internal friction angle | - |
| $C_d$ | Drag coefficient of a sand particle | - |
| $D$ | Grain diameter | m |
| $I$ | Inertial number | - |
| $I_0$ | Numerical constant | - |
| $\boldsymbol{M}_m$ | Influence of the surface tension force on the mixture | $\mathrm{N/m^3}$ |
| $Re_p$ | The Reynolds number for an isolated suspended particle | - |
| $c$ | Cohesion | $\mathrm{N/m^2}$ |
| $\boldsymbol{j}$ | Volumetric flux | $\mathrm{m/s}$ |
| $n$ | Richardson-Zaki hindered sedimentation exponent | - |
| $p_m$ | Mixture pressure | Pa |
| $\boldsymbol{u}_k$ | Velocity of phase $k$ | $\mathrm{m/s}$ |
| $\boldsymbol{u}_m$ | Centre of gravity velocity | $\mathrm{m/s}$ |
| $\boldsymbol{v}_{dk}$ | Drift-flux of phase k | $\mathrm{m/s}$ |
| $w_0$ | Settling velocity for $\alpha_d = 0$ | $\mathrm{m/s}$ |
| $_c$ | Of the continuous phase (e.g. water) | |
| $_d$ | Of the dispersed phase (e.g. sand) | |
| $_m$ | Of the mixture | |